Electrodeposition and Characterization of Conducting Polymer Films Obtained from Carbazole and 2-(9H-carbazol-9-yl)acetic Acid

Sophie Lakard, Emmanuel Contal, Karine Mougin, Boris Lakard

electrochem

MDPI

Article

Electrodeposition and Characterization of Conducting Polymer Films Obtained from Carbazole and 2-(9H-carbazol-9-yl)acetic Acid

Sophie Lakard [1], Emmanuel Contal [1], Karine Mougin [2] and Boris Lakard [1,*]

[1] Institut UTINAM UMR CNRS 6213, University Bourgogne Franche-Comté, 16 Route de Gray, 25030 Besançon, France; sophie.lakard@univ-fcomte.fr (S.L.); emmanuel.contal@univ-fcomte.fr (E.C.)
[2] Institut de Science des Matériaux, Université de Haute Alsace, IS2M-CNRS-UMR 7361, 15 Rue Jean Starcky, 68057 Mulhouse, France; karine.mougin@uha.fr
* Correspondence: boris.lakard@univ-fcomte.fr; Tel.: +33-381-662-046

Abstract: Electrochemical oxidation of electrolyte solutions containing carbazole (Cz) and 2-(9H-carbazol-9-yl)acetic acid (CzA) monomers was performed in acetonitrile solutions. Different Cz and CzA feed ratios were used to electrodeposit solid polymer films of various compositions, and to study the influence of the monomer ratio on the physicochemical properties (electroactivity, topography, adhesion, stiffness, wettability) of the polymer films. Thus, electrochemical oxidation led to the deposition of a solid film of micrometric thickness, but only for the solutions containing at least 30% of Cz. The proportion of Cz and CzA in the electrodeposited polymer films has little impact on the adhesion strength values measured by AFM. On the contrary, this proportion significantly modifies the stiffness of the films. Indeed, the stiffness of the polymer films varies from 9 to 24 GPa depending on the monomer ratio, which is much lower than the value obtained for unmodified polycarbazole (64 GPa). This leads to the absence of cracks in the films, which all have a fairly homogeneous globular structure. Moreover, among the different polymer films obtained, those prepared from 70:30 and 50:50 ratios in Cz:CzA monomer solutions seem to be the most interesting because these green films are conductive, thick, low in stiffness, do not show cracks and are resistant to prolonged immersion in water.

Keywords: electrochemistry; carbazole; conducting polymers; physico-chemistry; stiffness; adhesion

Citation: Lakard, S.; Contal, E.; Mougin, K.; Lakard, B. Electrodeposition and Characterization of Conducting Polymer Films Obtained from Carbazole and 2-(9H-carbazol-9-yl)acetic Acid. *Electrochem* **2022**, *3*, 322–336. https://doi.org/10.3390/electrochem3020022

Academic Editor: M'hamed Chahma

Received: 19 May 2022
Accepted: 16 June 2022
Published: 17 June 2022

1. Introduction

Conducting polymers are a class of materials whose conductive properties were first demonstrated in 1977 with the discovery of electrically conducting polyacetylene by Shirakawa, MacDiarmid, and Heeger [1]. Although polyacetylene is a very highly conductive (up to 10^5 S/cm) polymer, its high instability in air due to oxidative degradation by oxygen [2] and at elevated temperatures [3] has limited its commercial potential. Therefore, other intrinsically conducting polymers, including polypyrrole [4,5], polyaniline [6,7], polythiophene [8,9], polyfuran [10,11], polycarbazole [12,13], and others, have been prepared and are widely used due to their remarkable electrical and optical properties as well as good stability. Thus, these polymers are used for a large number of applications such as: supercapacitors and energy storage [14,15], (bio) fuel cells [16,17], anticorrosion [18,19], gas sensors [20,21], biosensors [22,23], or tissue engineering [24,25].

In particular, carbazole and its derivatives are a class of heterocyclic conducting polymers that has attracted attention due to their excellent charge transport capacity, photoconductivity and electrochromic properties, their versatility in functionalization, and their good chemical and environmental stability [26], which has led to much work in the fields of photovoltaic devices [27–29], electrochromic devices [30,31], organic transistors [32,33], and biomedical applications [34,35].

Polycarbazoles can be prepared by chemical polymerization of carbazole derivatives in the presence of oxidizing agents such as ferric chloride, ammonium persulphate, and potassium dichromate. The structure and properties of the resulting polymers are dependent on the concentration, oxidizing agent, and solvent [36]. Polycarbazoles can also be obtained by electropolymerization, which consists of depositing a polymer film by anodic oxidation on a conductive surface such as a noble metal (gold, platinum), glassy carbon, ITO or FTO (indium or fluorine tin oxide) [37,38]. To improve the solubility of the monomers and the electrical and optical properties of the polymers, carbazole monomers are often functionalized by grafting chemical groups leading to soluble carbazole derivatives that can be polymerized by (electro)chemical oxidation. Oxidation of carbazoles can occur at different positions since carbazoles have several active positions (3,6-, 2,7-, and 1,8-positions). Among them, the 3,6 carbazole derivatives are the most studied, since these positions are the easiest to oxidize [36]. Oxidation of 2,7-carbazoles can also lead to polymers with extended conjugation and low band gap [39]. On the contrary, poly(1,8-carbazole) derivatives are the least studied because these polymers are less planar than 3,6 and 2,7, which limits their applicability [40].

The carboxyl group is certainly one of the most interesting chemical groups to add to carbazole to make it sensitive to the pH of the medium, to give it complexing properties, to modify its wettability, electrochemical and optical properties, or to promote its interaction with biological media. For example, a complex, based on a novel organotin(IV) complex with 9-hexyl-9H-carbazole-3-carboxylic acid was tested in vitro for its cytotoxic activity, using a hepatocellular carcinoma cell line, and showed greater cytotoxicity than that of 5-fluorouracil which was used as a positive control substance [41]. In addition, the electrodeposition of poly(4-methyl carbazole-3-carboxylic acid) was successfully performed on stainless steel surfaces by Düdükcü et al. [42]. The corrosion tests indicated that this polymer provided effective anodic protection of steel surfaces in a corrosion test solution. Additionally, Elkhidr et al. successfully performed the electropolymerization of carbazol-9-yl-carboxylic acid in acetonitrile. The electro-generated polycarbazole films exhibited remarkable redox activity and electrochromic properties with increasing potential, which were explained in detail using spectroelectrochemical studies [43]. Kuo et al. electrodeposited three copolymers based on carbazole and indole-6-carboxylic acid (In) on an ITO surface [44]. These films were used as electrochromic materials in electrochromic devices and the polymer with a Cz/In feed molar ratio of 4:1 showed the highest contrast and coloring efficiency. The latter example is also interesting since it combines functionalization and copolymerization of carbazole and indole. Indeed, one way to improve the properties of polycarbazoles is to prepare copolymer films combining carbazole units with other units. Similarly, copolymers have been synthesized by polymerization of indolo [3,2-b]carbazole, isoindigo and thiophene units [45]. The incorporation of different alkyl-branched units facilitated the improvement of optical properties, solubility, conjugate structure, and electrochromic performance (fast bleaching/coloration response time, high coloration efficiency, and stable optical contrast). Recently, the electrochemical synthesis of copolymers from a carbazole–thiophene unit was reported by Aristizabal et al. [46]. This work highlighted the dependence of the structure of the generated polymer on the applied potential since a low potential facilitated the connection between the carbazole rings, and a high potential favors the incorporation of the thiophene rings. The same authors recently reported the electrochemical polymerization of an original carbazole-thiophene unit substituted with an alkyl chain in position 3, which sterically inhibited one of the processes that occur due to a high potential and resulted in the formation of a material with a more regular structure [47]. In another study, electrochemical copolymerization of carbazole derivatives and ethylenedioxythiophene (EDOT) led to the formation of original materials with electrochromic properties between black and transparent [48]. Similarly, Aydin et al. electropolymerized copolymers of carbazoles with thiophene, EDOT and pyrrole [49]. The obtained compounds showed sufficiently interesting spectroelectrochemical and electrochromic properties to be considered as potential organic solar cell materials.

In a previous study, our group also electrodeposited polymer films from carbazole and N-((methoxycarbonyl)methyl)carbazole monomers. Depending on the ratio of the feed monomers, these films showed very different morphological features and stiffness [50].

Considering this literature, it appears that if polycarbazoles possess remarkable electrical and optical properties, it is, however, sometimes necessary to functionalize them or to combine several monomers to introduce additional chemical groups allowing to improve their chemical reactivity, their mechanical resistance, or other physicochemical properties. Thus, in this work, we sought to electrodeposit polymer films by oxidation of carbazole and 2-(9H-carbazol-9-yl)acetic acid monomers (Figure 1) in order to: (i) prepare solid films with improved mechanical stability, (ii) integrate carboxyl functions inside the films. Indeed, the presence of carboxyl groups is likely to allow the formation of peptide bonds with biological cells or enzymes thanks to the presence of amine groups in these compounds, which opens prospects for the development of biosensors or biomaterials. Similarly, the presence of carboxyl groups can promote the formation of hydrogen bonds or generate electrostatic interactions (if ionized) within the film, thus causing changes in the structure or rigidity of the films.

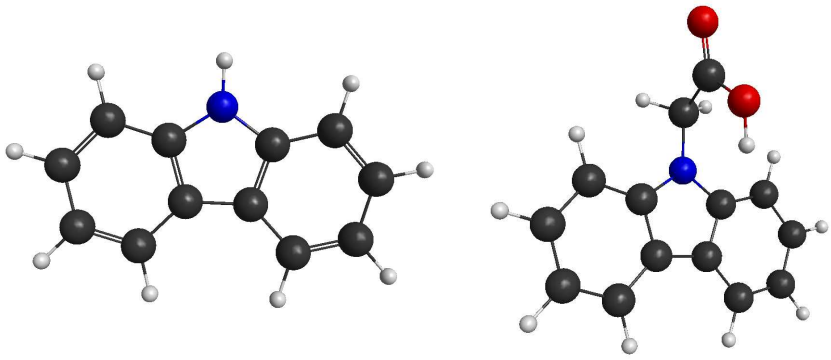

(**a**) (**b**)

Figure 1. Structure of carbazole (**a**) and 2-(9H-carbazol-9-yl)acetic acid (**b**).

2. Materials and Methods

2.1. Materials and Reagents

Carbazole (>95%, Cz) and lithium perchlorate (>95%, LiClO4) were purchased from Sigma Aldrich when acetonitrile (>99.5%, ACN) was purchased from Fisher Scientific. The electrolytic solution was composed of carbazole and 2-(9H-carbazol-9-yl)acetic acid (CzA) used as co-monomers, $LiClO_4$ as supporting salt, and ACN as solvent. CzA was synthesized in the lab following a procedure that has already been reported in detail [50,51]. All the chemical reagents used to synthesize the CzA product were from Sigma-Aldrich.

2.2. Electrodeposition of Polymer Films

Electrochemical experiments were performed in a standard three-compartment electrochemical cell using either a platinum wire (0.785 mm^2) or a fluorine-doped tin oxide (FTO) substrate (10 mm × 30 mm, thickness: 1.1 mm, R = 80 Ω/square, from Solems) as the working electrode, a saturated calomel electrode (SCE) as the reference electrode, and a Pt sheet as the counter-electrode.

Electrolytic solutions were prepared from a Cz solution, a solution CzA, or a mixture of Cz and CzA with the following molar ratios of Cz:CzA: 95:5, 90:10, 70:30, 50:50, 30:70, 10:90 and 5:95. For example, the polymer film denoted Cz70-CzA30 was prepared by electrochemical oxidation of an electrolytic solution obtained by adding 14 mL of a solution of acetonitrile with 0.1 M lithium perchlorate and Cz (10^{-2} M) to 6 mL of a solution of acetonitrile with 0.1 M lithium perchlorate and CzA (10^{-2} M). All electrochemical experiments were performed at room temperature with a VersaSTAT MC potentiostat/galvanostat

from Princeton Applied Research. Polymer films were electropolymerized either by cyclic voltammetry on a platinum working electrode in a potential range of 0.0 to +2.0 V/SCE and a scan rate of 50 mV/s, or by chronoamperometry on a FTO electrode at a potential of +1.5 V/SCE for 3 min.

2.3. Characterization Techniques

AFM microscopy. The analysis of electrodeposited polymer films was performed with a Bruker Multimode 8 AFM equipped with the Peakforce Quantitative Nanomechanics (PeakForce QNM) mode [52]. This mode is a recent advancement in AFM technique that provides a quantitative nanomechanical mapping mode with simultaneous measurement of tip-to-surface adhesion, Young's modulus (according to the DMT or Sneddon model), and surface topography. Etched silicon QNM probes RTESPA-300 (from Bruker), with a nominal spring constant k $\approx$ 40 N/m, were used for all AFM experiments. Nanoscope analysis 1.9 and Gwyddion softwares were used to determine the DMT modulus and average adhesion of samples from at least three representative AFM images from different areas of each sample.

SEM microscopy. The topography of the polymer films was studied, without prior metallization, using a FEI Quanta 450 W high resolution SEM microscope. The electron beam energy used was 12.5 keV and the working distance used was between 9 and 12 mm.

2.4. Theoretical Calculations

The solvent free energy of the Cz and CzA monomers was calculated using the open-source software package GAMESS (General Atomic and Molecular Electronic Structure System) developed at Iowa State University. After an initial optimization of the starting geometries using the semi-empirical PM3 approach [53], calculations were performed using the B3LYP method (combined with a 6-31G* basis set), which is a DFT (Density Functional Theory) method involving the gradient correction of the Becke exchange functional [54] and the Lee-Yang-Parr correction functional [55] and is appropriate for modeling π-conjugation systems due to the inclusion of electron correlation effects [56–58]. Moreover, the Polarizable Continuum Model (PCM) can be used in combination with the previous methods in order to calculate the total free energy of monomers in acetonitrile because this solvation model provides a realistic description of the molecular shape by constructing the solute cavity from a union of atom-centered spheres. Thus, the solvent free energy of the monomers and their corresponding radical cations was calculated using the DFT method and the PCM model, and the Gibbs free energy of activation of the oxidation reactions leading from the monomers to the radical cations was deduced from these calculations. A Gibbs free energy of activation of +5.443 eV was obtained for the oxidation of Cz to its radical cations ($\Delta G_{Cz\neq} = G_{Cz+} - G_{Cz}$ = $-14{,}066.933 - (-14{,}072.376)$ = +5.443 eV) when a value of +5.633 eV was obtained for the oxidation of CzA ($\Delta G_{CzA\neq} = G_{CzA+} - G_{CzA}$ = $-20{,}264.384 - (-20{,}270.017)$ = +5.633 eV).

3. Results

3.1. Electropolymerization of Carbazole and 2-(9H-carbazol-9-yl)acetic Acid:

The oxidation of carbazole (10^{-2} M) and 2-(9H-carbazol-9-yl)acetic acid (10^{-2} M) is performed by cyclic voltammetry at a platinum electrode by applying five potential sweeps between 0 and +2 V/SCE, with a scan rate of 50 mV/s, in an acetonitrile solution containing 0.1 M $LiClO_4$. The potential of the oxidation peak of Cz monomers, leading to radical cations, appears at +1.1 V/SCE (Figure 2a), while that of CzA monomers appears at a higher potential value of +1.5 V/SCE (Figure 2b). Thus, the cyclic voltammograms demonstrate that the oxidation of Cz monomers is easier than the one of CzA monomers, which is confirmed by the calculated values of the Gibbs free energy of activation of the monomer oxidation. Indeed, the Gibbs free energy of activation of the oxidation of CzA into its radical cation (+5.633 eV) is higher than the one of Cz (+5.443 eV) by 0.190 eV, which confirms that the oxidation of CzA is energetically less favorable that the oxidation of Cz.

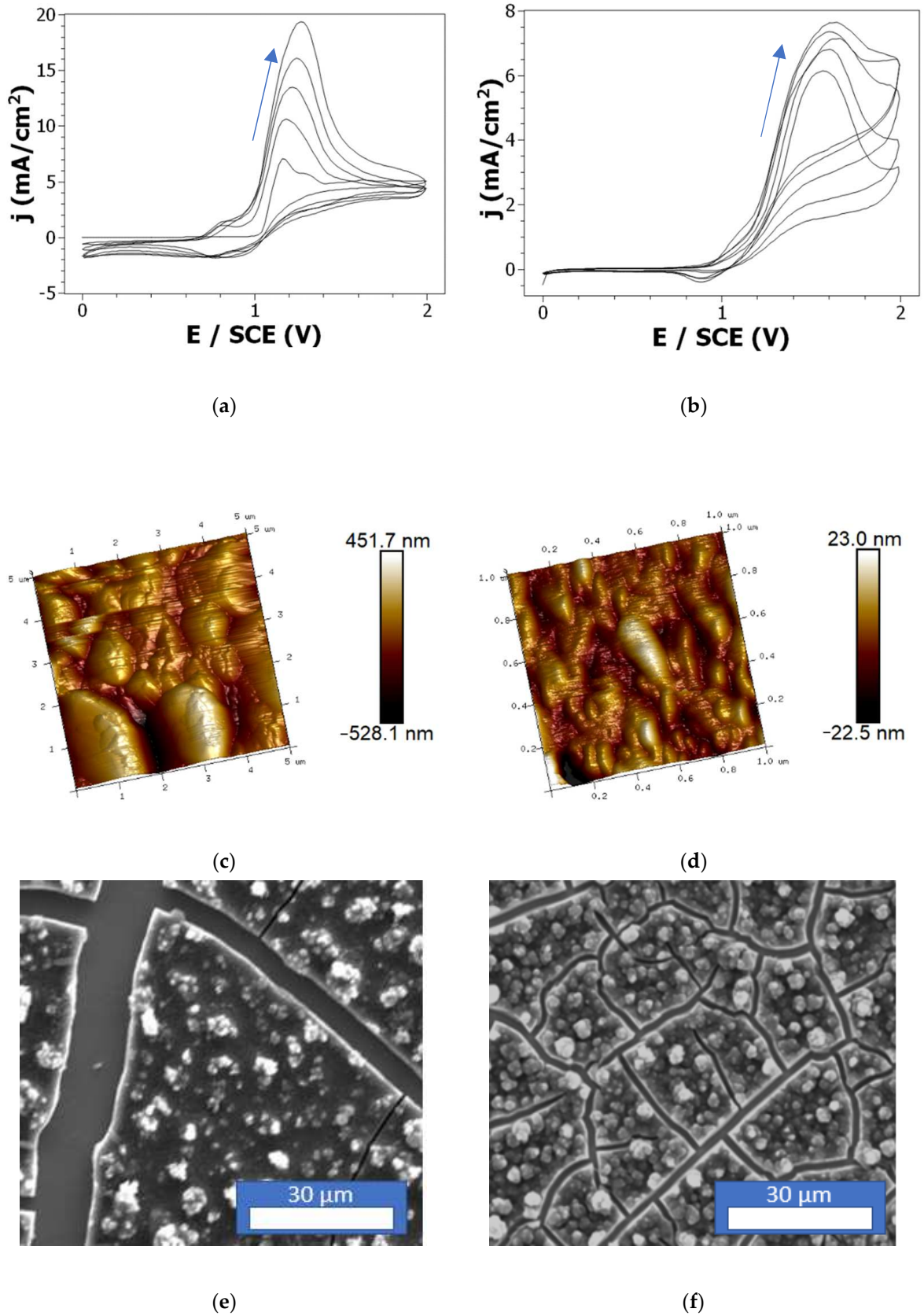

Figure 2. Cyclic voltammetry of 10^{-2} M Cz (**a**) or CzA (**d**) in 0.1 M $LiClO_4$/ACN at a Pt electrode with a scan rate of 50 mV/s. Three-dimensional morphology AFM (**b**,**e**) and SEM (**c**,**f**) images of the PCz and PCzA films electrodeposited on a FTO substrate (chronoamperometry at +1.5 V/SCE, 3 min).

Moreover, for both monomers, the current density of the monomer oxidation peak reaches about 6 mA/cm^2 during the first potential scan. During the following cycles, the current density of the oxidation peak of Cz increases progressively to reach 20 mA/cm^2 during the 5th cycle, whereas the current density of the oxidation peak of CzA increases very slightly to reach only 8 mA/cm^2 during the 5th cycle. In addition, two smaller peaks are visible from the second scan at +0.8 and +0.75 V/SCE, which correspond to the oxidation and reduction peaks of the electrodeposited polycarbazole film, respectively (PCz, Figure 2a). Similarly, these small peaks are visible from the second scan at +1.0 and +0.9 V/SCE in Figure 2b, showing that the substituted polycarbazole film (polyCzA) is also electroactive. Indeed, these redox peaks are the evidence of the electroactivity of the polymer films since the oxidation peak can be associated with both the polymer oxidation and the insertion of counter-anions into the polymer film, and the reduction peak with the polymer reduction and the ejection of counter-anions from the polymer film. The current increases with the cycles in the case of Cz, showing that it is a conductive polymer, easier to oxidize as the polymer chain grows due to the strong conjugation in the polymer backbone. The current also increases in the case of CzA, but less markedly due to the presence of carboxyl groups that can partially break the conjugation within the polymer film.

After that, a potential of + 1.5V/SCE is applied during 3 min in the monomer solutions to electrogenerate a thick polymer film by potentiostatic electrodeposition onto a transparent FTO electrode. The PCz film resulting from this electrodeposition process is thick and dark green-colored to the eye. On the contrary, the PCzA film appears as a very thin film and is difficult to observe with the eye (Figure 3). The morphology of the PCz film consists in micrometric globules as demonstrated by the AFM image (Figure 2c). The morphology of the PCzA film is also composed of globules that are a little smaller (Figure 2d), but the PCzA film is greatly thinner than the PCz one since the maximum peak-to-valley height observed in the AFM image is ≈50 nm for the PCzA and ≈1 µm for the PCz one.

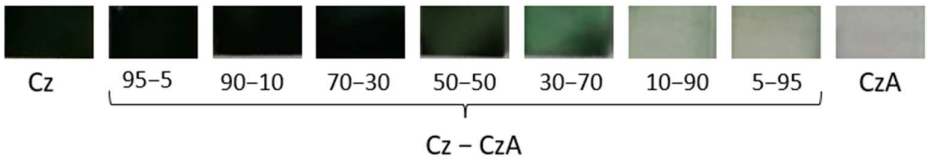

Figure 3. Pictures of polymer films obtained by electro-oxidation of Cz and CzA monomers.

The Young modulus of the polymer film was also measured through AFM measurements as well as the AFM force adhesion measured between the polymer film and the AFM tip. The average force adhesion value is 20 ± 5 nN for PCz film, while it is 34 ± 5 nN for PCzA film. More interestingly, the Young modulus of both polymer films are very high since it reaches 64 GPa for PCz and 30 GPa for PCzA. These high values of the Young modulus evidence that these electrodeposited PCz and PCzA films have a high stiffness, which is certainly responsible from the cracks observed in the SEM images (Figure 2c,f, respectively). Consequently, it is important to find a solution allowing us to electrogenerate polycarbazole films with less cracks and enhance their mechanical properties. A possible strategy to obtain polymer films with such properties is to perform the simultaneous polymerization of Cz and CzA monomers on the same working electrode.

3.2. Theoretical and Electrochemical Study of the Oxidation of Mixtures of Cz and CzA:

3.2.1. Coupling between Oxidized Monomers

As demonstrated by Ambrose et al. the electropolymerization of carbazole begins with the oxidation of carbazole to an unstable cationic radical that couples with another cationic radical to form the most stable dimer, which is 3,3′-bicarbazyl [59]. Then, the oxidation of this dimer takes place and the polymer chain gradually grows to form a solid film on the electrode surface. The electrochemical oxidation of 9-substituted carbazoles, such as CzA, occurs similarly to that of carbazole and leads to the formation of 3,3′-bicarbazyl all the more easily since the 9-position is already occupied and cannot give rise to coupling [60,61].

Therefore, the polymerization of the Cz and CzA mixtures can be expected to occur by 3-3′ coupling of the monomers. In order to support this hypothesis, the free energy in the solvent of the dimer obtained by 3,3′ coupling was calculated and compared to that of other dimers that could be obtained by coupling of Cz and CzA (Table 1). The results obtained indeed confirm that the most stable dimer corresponds to the 3-3′ coupling ($G_{3\text{-}3'}$ = −34,116.538 eV). It is also likely that the subsequent growth of the polymer film is carried out according to successive 3-3′ couplings. The optimized chemical structure of the dimer coupled at the 3 and 3′ positions is given in Figure 4.

Table 1. Total free energy in solvent (in eV) of the different dimers that can be formed by coupling between Cz and CzA monomers. Calculations performed using the B3LYP DFT method with the 6-31G* basis set and the PCM model that includes solvent effects.

Coupling Leading to a Dimer (Cz-CzA Coupling)	$G_{Cz\text{-}CzA}$ (in eV)
9-1′ coupling	−34,115.830
9-3′ coupling	−34,116.021
3-1′ coupling	−34,116.374
1-1′ coupling	−34,116.402
1-3′ coupling	−34,116.483
3-3′ coupling	−34,116.538

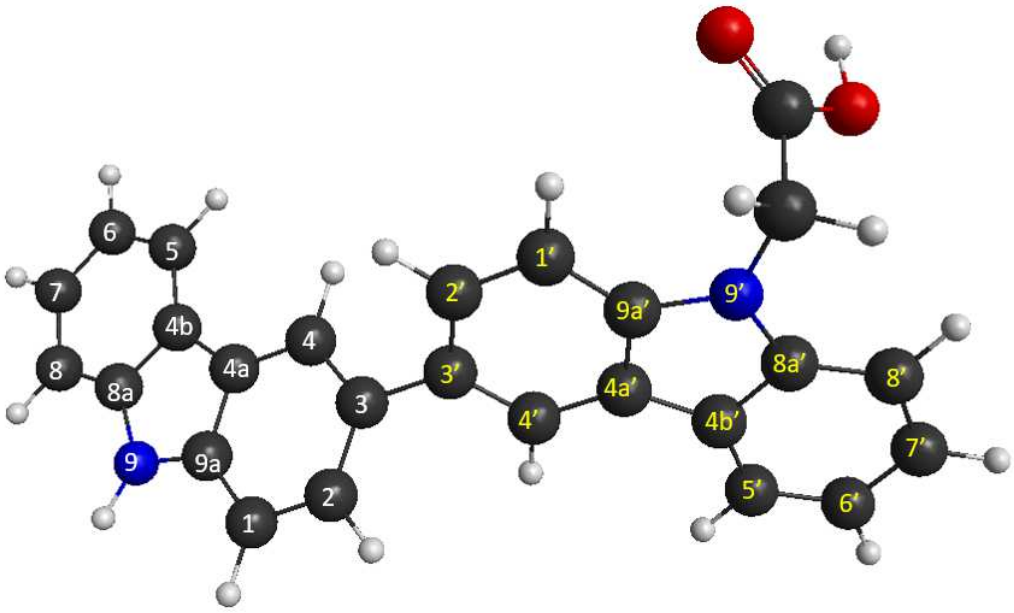

Figure 4. Representation of the chemical structure of 3,3′-CzCzA dimer (deduced from DFT calculations at the B3LYP/6-31G* level of theory).

3.2.2. Electrochemical Polymerization of Mixtures of Cz and CzA: Polymers with a High Portion of Cz Monomers

Oxidation of monomer solutions containing Cz:CzA ratios of 95:5 and 90:10 is carried out at a platinum electrode in a 0.1 M $LiClO_4$/acetonitrile solution. The CVs obtained are similar to those obtained by oxidation of Cz monomers. Indeed, a pronounced anodic peak is visible at +1.1 V/SCE (Figure 5a,b) in the first scan that can be mainly attributed to the oxidation of Cz monomers rather than to the CzA monomers which are less numerous and whose oxidation peak is located at higher potential (Figure 2d). In subsequent scans, the electropolymerization reaction continues as demonstrated by the gradual increase of the current density with repeated potential scans. Furthermore, both resulting polymer films are electroactive since an anodic and a cathodic peak due to the redox process and the insertion and de-insertion of counter-anions taking place in the polymer film are

visible at +0.7–0.8 V/SCE. At the end of the CV, a thick dark green solid film can be observed on the surface of the Pt electrode. A similar green coating is also visible after potentiostatic deposition of the polymer film on the FTO substrate (Figure 3). Therefore, the electrochemical behavior obtained with these ratios is very similar to that obtained with Cz. The AFM topography (Figure 5c,d) confirms the similarity between these polymer films since they all have the same granular structure and comparable thickness (since the maximum peak-to-valley height is between 1.2 and 1.6 µm), and the force adhesion between the film and the AFM tip are almost equals (19–22 nN). On the contrary, it is really interesting to note the absence of cracks on the polymer films in the SEM images (Figure 6) when the polymer film contains both Cz and CzA monomers. This absence of cracks is certainly due to a lower internal stress, which leads to a lower Young's modulus (13–18 GPa) compared to those of the PCz film (64 GPa) and the PCzA film (30 GPa).

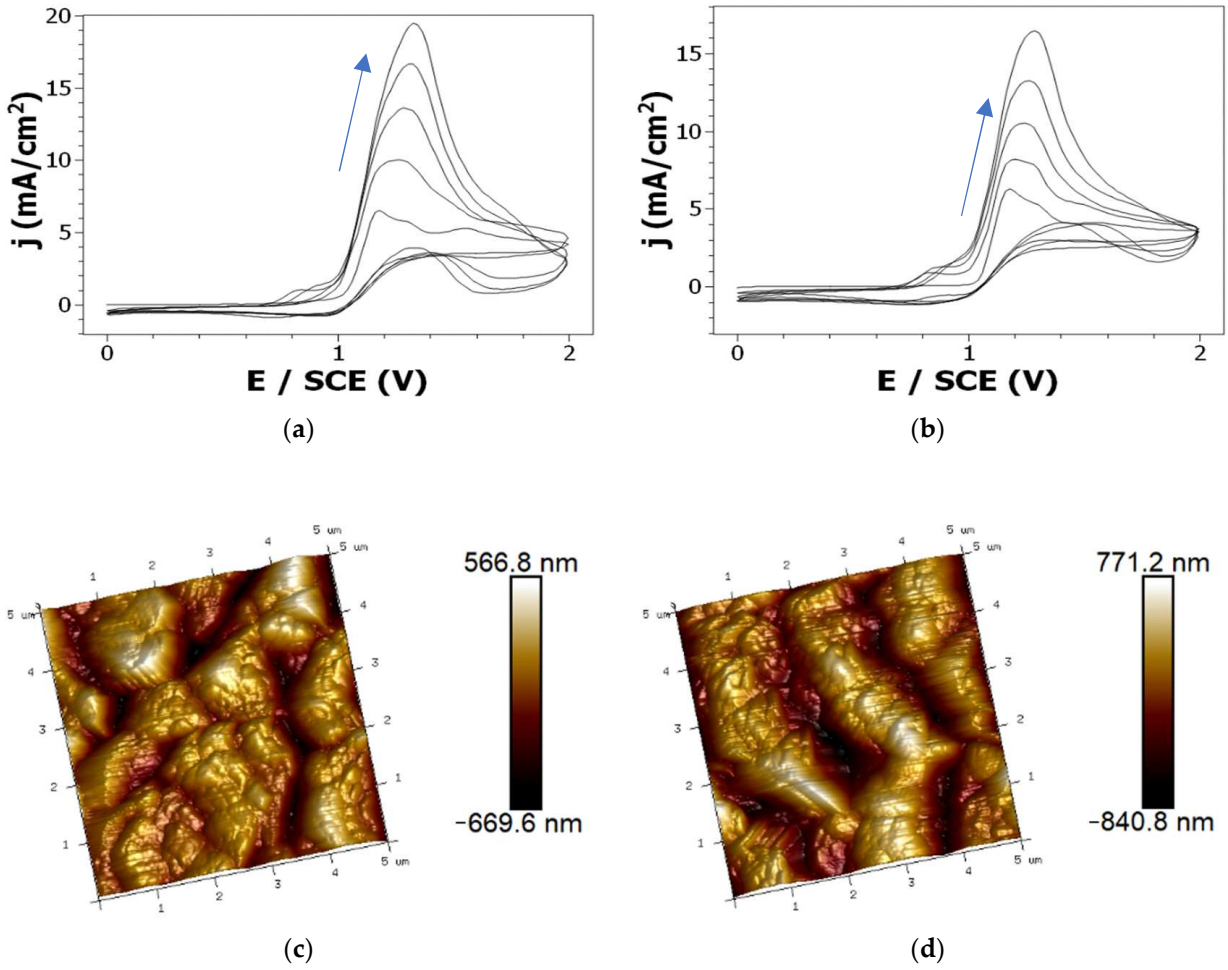

Figure 5. Cyclic voltammograms obtained by oxidation of: 95:5 Cz:CzA (**a**) or 90:10 Cz:CzA (**b**) in an acetonitrile + 0.1 M $LiClO_4$ solution (WE: Pt. Scan rate: 50 mV/s) and 3D morphology AFM pictures of the polymer films resulting from the electro-oxidation of 95:5 Cz:CzA (**c**) and 90:10 Cz:CzA (**d**) solutions.

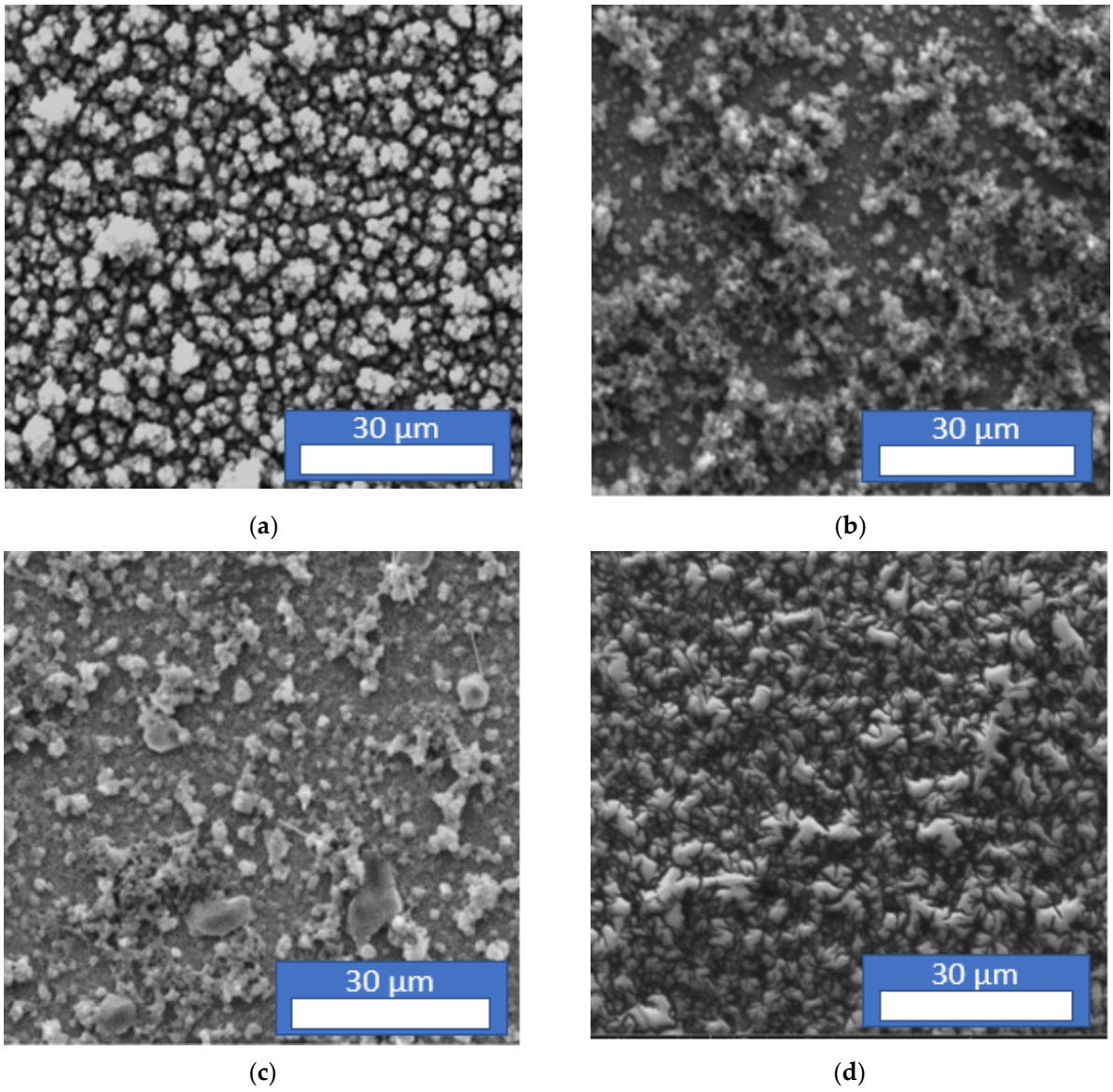

Figure 6. SEM pictures of the polymer films resulting from the electro-oxidation of 95:5 Cz:CzA (**a**), 70:30 Cz:CzA (**b**), 50:50 Cz:CzA (**c**), and 5:95 Cz:CzA (**d**) solutions.

Polymers with a Balanced Portion of Cz and CzA Monomers

Oxidation of monomer solutions containing Cz:CzA ratios of 70:30, 50:50 and 30:70 is then performed under the same conditions as before. The oxidation peak that was present for high carbazole ratios is still visible at +1.2–1.3 V/SCE (Figure 7a–c). In the first scan, the current density of the oxidation peak is between 5 and 6 mA/cm^2 for all three ratios as it was for the two monomers alone. On the contrary, in the following scans, the current density of this oxidation peak differs from one ratio to another since it increases up to 12 mA/cm^2 for the 70–30 Cz:CzA ratio while it does not exceed 8 mA/cm^2 for the 50:50 and 30:70 Cz:CzA ratios. Potentiodynamic or potentiostatic electro-oxidation of 70:30 and 50:50 Cz:CzA ratios leads to the formation of green films as dark as those previously deposited. On the contrary, the green film electrodeposited from the 30:70 ratio is light green and it does not seem to be as homogeneous as the other films (Figure 3).

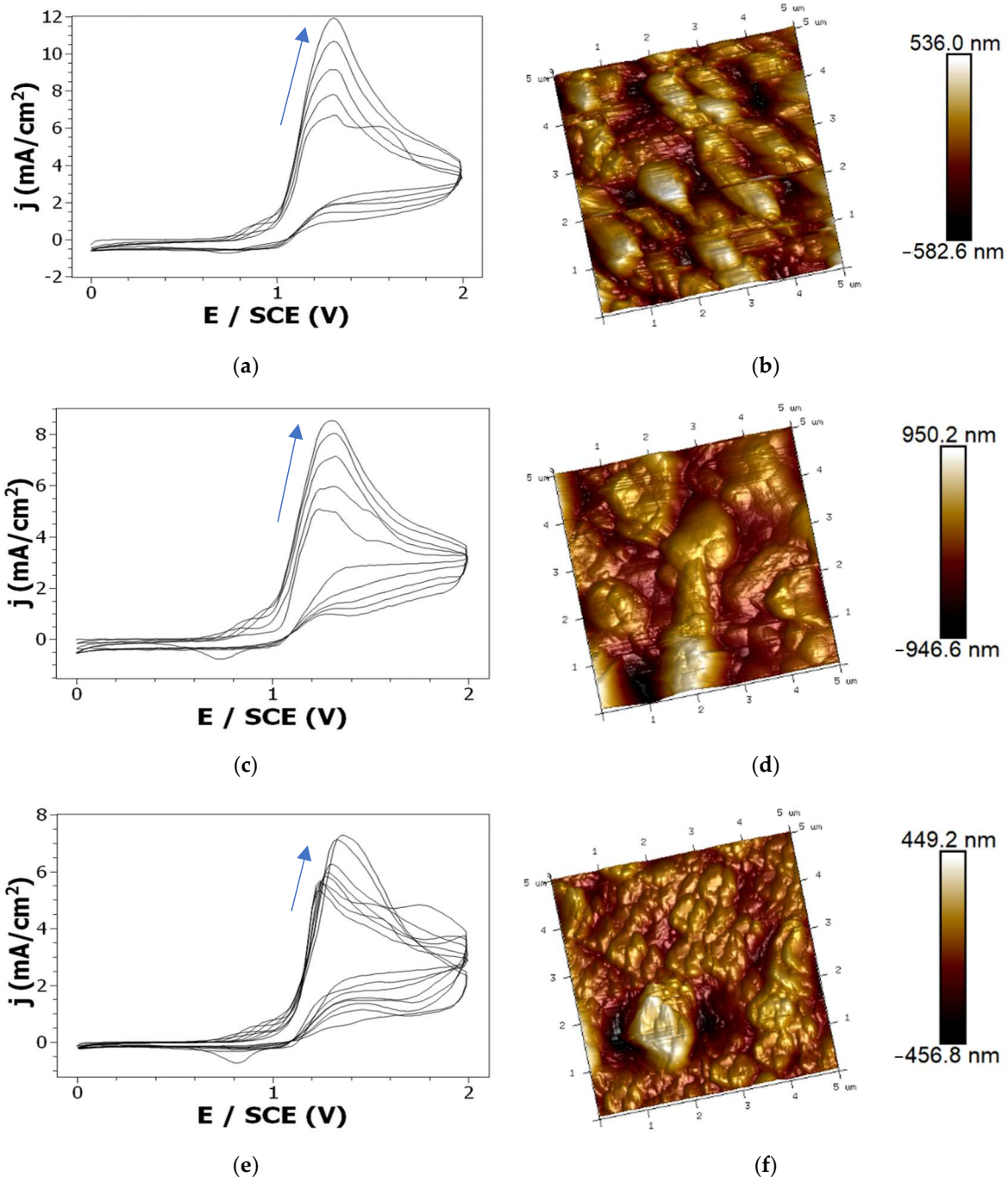

Figure 7. Cyclic voltammograms obtained by oxidation of: 70:30 Cz:CzA (**a**), 50:50 Cz:CzA (**b**) and 30:70 Cz:CzA (**c**) in an acetonitrile +0.1 M $LiClO_4$ solution (WE: Pt. Scan rate: 50 mV/s) and 3D morphology AFM pictures of the polymer films resulting from the electro-oxidation of 70:30 Cz:CzA (**d**), 50:50 Cz:CzA (**e**) and 30:70 Cz:CzA (**f**) solutions.

The films obtained from the 70:30 (Figure 6b) and 50:50 Cz:CzA (Figure 6c) ratios are particularly interesting since they have a lower Young modulus (9 GPa) than the other polymer films (Figure 6a,d) so that their structure does not show cracks as shown by the SEM images. Moreover, the polymers obtained from the 70:30 and 50:50 Cz:CzA ratios look like island structures achieved by a macromolecular nucleation mechanism. These results are similar to other studies that provide evidence of nucleation and three-dimensional growth for some electronically conducting polymers [62–64]. In addition, the 3D morphology AFM images show a globular structure. Furthermore, the adhesion force

(25–26 nN) of these films is comparable to that of the previous films studied as well as their thickness since their maximum peak-to-valley height is between 1 and 2 µm. On the contrary, while the film obtained from 30:70 Cz:CzA has a low Young modulus (13 GPa), the inhomogeneity of the film and the lower maximum height (0.9 µm) make it less interesting.

Polymers with a Low Portion of Cz Monomers

Finally, oxidation of monomer solutions containing Cz:CzA ratios of 10:90 and 5:95 is carried out in a 0.1 M $LiClO_4$/acetonitrile solution. A pronounced oxidation peak with a current density of 6 mA/cm^2 is visible at +1.1–1.2 V/SCE (Figure 8a,b). During subsequent scans, no increase in current density with repeated potential scans is observed indicating that the electropolymerization reaction is more difficult with these Cz:CzA ratios due to the low proportion of Cz monomers. Potentiodynamic or potentiostatic electro-oxidation of these mixtures leads to an extremely thin deposit since their maximum peak-to-valley height is 200 nm for the 90:10 Cz:CzA ratio and 30 nm for the 95:5 Cz:CzA ratio. Thus, the electrodeposited film is almost invisible to the naked eye on the surface of the FTO electrodes whereas previous mixtures led to thicker green deposits (Figure 3). AFM images confirm that these films are different from the previous ones (Figure 8c,d). Indeed, if these films also have a granular structure, the size of the grains is much smaller (less than 0.1 µm, except some rare aggregates) for these deposits than for the previous ones where some grains exceeded the micrometer. In addition, the Young's moduli of the films obtained from the Cz:CzA ratios of 10:90 and 5:95 are higher (17–24 GPa) than those obtained from the other mixtures. As shown previously, these high values indicate a film stiffness that is not desired, as it may lead to the formation of cracks. Moreover, the SEM image of the coating obtained from a Cz:CzA ratio of 5:95 contains some features that could be incipient cracks (Figure 6d).

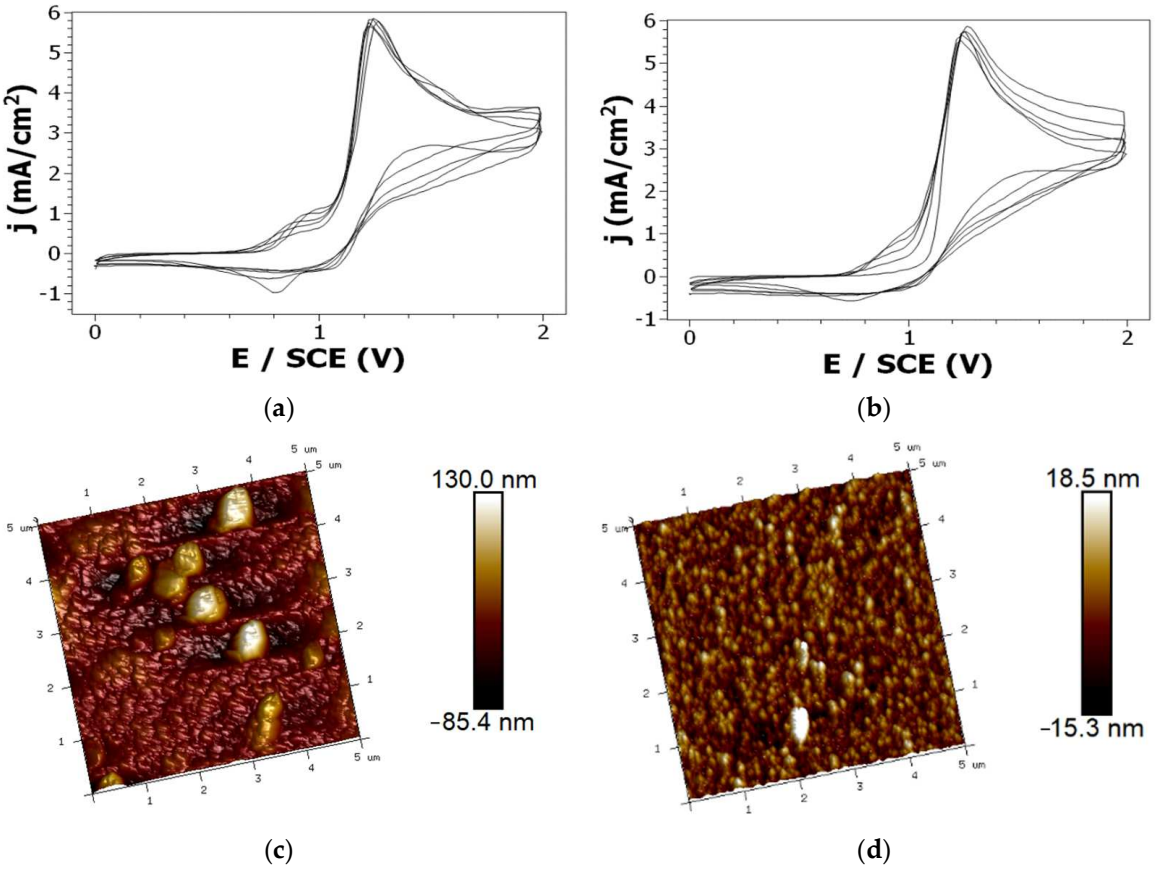

Figure 8. Cyclic voltammograms obtained by oxidation of: 10:90 Cz:CzA (**a**) or 5:95 Cz:CzA (**b**) in an acetonitrile + 0.1 M $LiClO_4$ solution (WE: Pt. Scan rate: 50 mV/s) and 3D morphology AFM pictures of the polymer films resulting from the electro-oxidation of 10:90 Cz:CzA (**c**) or 5:95 Cz:CzA (**d**) solutions.

Table 2 summarizes and compares the physico-chemical properties of the films obtained from the different Cz and CzA mixtures as well as PCz and PCzA films. It appears in this table that the most interesting mixtures correspond to the Cz:CzA ratios of 70:30 and 50:50 because they allow to obtain thick green films which are electroactive, globular but without cracks thanks to a low Young's modulus, a high adhesion force, and allow the insertion of carboxylic functions in the polymer films. Therefore, due to their electrical and mechanical properties, but also to the presence of carboxyl groups, these films could be used in the future as sensitive layers of (electro)chemical biosensors, as biomaterials or for other applications.

Table 2. Comparison of the physico-chemical properties of the films obtained by oxidation of Cz, CzA and Cz:CzA mixtures (in green: beneficial properties, in red: adverse properties, in black: neutral properties).

	Aspect (Naked-Eye)	Young Modulus (AFM)	Topography (AFM, SEM)	Intensity (CV)	Insertion of Carboxyl Groups
Cz	Green, Thick	High	Globular, cracks	High	No
Cz_{95}-CzA_5	Green, very thick	Medium/High	Globular, no crack	High	Yes
Cz_{90}-CzA_{10}	Green, very thick	Medium/Low	Globular, no crack	High	Yes
Cz_{70}-CzA_{30}	Green, very thick	Low	Globular, no crack	High	Yes
Cz_{50}-CzA_{50}	Green, very thick	Low	Globular, no crack	Medium	Yes
Cz_{30}-CzA_{70}	Light green, thick	Medium/Low	Globular, no crack	Medium	Yes
Cz_{10}-CzA_{90}	Colourless, very thin	Medium/High	Globular	Low	Yes
Cz_5-CzA_{95}	Colourless, very thin	Medium/High	Globular	Low	Yes
CzA	Colourless, very thin	High	Globular, cracks	Medium	Yes

4. Conclusions

Electrochemical oxidation of mixtures of carbazole and 2-(9H-carbazol-9-yl)acetic acid enabled the preparation of polymer films by both cyclic voltammetry and chronoamperometry. The ratio of Cz:CzA monomers had a significant impact on the electroactivity, thickness, morphology, and stiffness of the electrodeposited polymer films. In particular, the polymer films with high Young's modulus showed cracks in their structure, while the polymer films with low Young's modulus exhibited an uncracked structure. Among all the Cz:CzA ratios studied, the 70:30 and 50:50 ratios are the most interesting because they are not cracked, have high electroactivity, and can easily form thick films while showing good adhesion to the substrate. Films with a higher proportion of Cz monomers are also interesting because they are very electroactive, even if their rigidity remains quite high. On the contrary, films obtained from mixtures containing more CzA monomers are difficult to electropolymerize, which does not allow us to obtain films of sufficient thickness to make them interesting for an application. In future studies, we hope to take advantage of the presence of carboxyl groups and the electrical and mechanical properties of the most promising polymer films to develop applications in the biomedical field. Indeed, the presence of these carboxyl groups should allow the fixation of biological compounds (cells, proteins, enzymes, amino acids) by the formation peptide bonds, making possible applications of these films as biomaterials or active layer of electrochemical biosensors.

Author Contributions: Methodology, S.L.; investigation, K.M., S.L. and E.C.; writing—review and editing, S.L., E.C., K.M. and B.L.; funding acquisition, B.L. All authors have read and agreed to the published version of the manuscript.

Funding: This research was partly funded by the Bourgogne Franche-Comté Regional Council through the COMICS (2019–2022) and MatElectroCap (2021–2024) projects. It was also supported by the French RENATECH network and its FEMTO-ST technological facility.

Institutional Review Board Statement: Not applicable.

Informed Consent Statement: Not applicable.

Data Availability Statement: Not applicable.

Conflicts of Interest: The authors declare no conflict of interest.

References

1. Shirakawa, H.; Louis, E.J.; MacDiarmid, A.G.; Chiang, C.K.; Heeger, A.J. Synthesis of electrically conducting organic polymers: Halogen derivatives of polyacetylene, (CH)x. *J. Chem. Soc., Chem. Commun.* **1977**, *16*, 578–580. [CrossRef]
2. Pochan, J.M.; Pochan, D.F.; Rommelmann, H.; Gibson, H.W. Kinetics of doping and degradation of polyacetylene by oxygen. *Macromolecules* **1981**, *14*, 110–114. [CrossRef]
3. Masuda, T.; Tang, B.Z.; Higashimura, T.; Yamaoka, H. Thermal degradation of polyacetylenes carrying substituents. *Macromolecules* **1985**, *18*, 2369–2373. [CrossRef]
4. Jain, R.; Jadon, N.; Pawaiya, A. Polypyrrole based next generation electrochemical sensors and biosensors: A review. *TRAC* **2017**, *97*, 363–373. [CrossRef]
5. Stejskal, J.; Trchová, M. Conducting polypyrrole nanotubes: A review. *Chem. Pap.* **2018**, *72*, 1563–1595. [CrossRef]
6. Liao, G.; Li, Q.; Xu, Z. The chemical modification of polyaniline with enhanced properties: A review. *Progr. Org. Coat.* **2019**, *126*, 35–43. [CrossRef]
7. Zare, E.N.; Makvandi, P.; Ashtari, B.; Rossi, F.; Motahari, A.; Perale, G. Progress in conductive polyaniline-based nanocomposites for biomedical applications: A review. *J. Med. Chem.* **2020**, *63*, 1–22. [CrossRef]
8. Kaloni, T.P.; Giesbrecht, P.K.; Schreckenbach, G.; Freund, M.S. Polythiophene: From fundamental perspectives to applications. *Chem. Mater.* **2017**, *29*, 10248–10283. [CrossRef]
9. Al-Refai, H.H.; Ganash, A.A.; Hussein, M.A. Polythiophene and its derivatives–Based Nanocomposites in Electrochemical Sensing: A Mini Review. *Mater. Today Com.* **2021**, *26*, 101935. [CrossRef]
10. Cao, H.; Rupar, P.A. Recent advances in conjugated furans. *Chem. Eur. J.* **2017**, *23*, 14670–14675. [CrossRef]
11. Yao, W.; Liu, P.; Liu, C.; Xu, J.; Lin, K.; Kang, H.; Li, M.; Lan, X.; Jiang, F. Flexible conjugated polyfurans for bifunctional electrochromic energy storage application. *Chem. Eng. J.* **2022**, *428*, 131125. [CrossRef]
12. Nayana, V.; Kandasubramanian, B. Polycarbazole and its derivatives: Progress, synthesis, and applications. *J. Polym. Res.* **2020**, *27*, 285. [CrossRef]
13. Bekkar, F.; Bettahar, F.; Moreno, I.; Meghabar, R.; Hamadouche, M.; Hernaez, E.; Vilas-Villa, J.L.; Ruiz-Rubio, L. Polycarbazole and its derivatives: Synthesis and applications. A review of the last 10 years. *Polymers* **2020**, *12*, 2227. [CrossRef] [PubMed]
14. Naskar, P.; Maiti, A.; Chakraborty, P.; Kundu, D.; Biswas, B.; Banerjee, A. Chemical supercapacitors: A review focusing on metallic compounds and conducting polymers. *J. Mater. Chem. A* **2021**, *9*, 1970–2017. [CrossRef]
15. Basnayaka, P.A.; Ram, M.K. A Review of Supercapacitor Energy Storage Using Nanohybrid Conducting Polymers and Carbon Electrode Materials. In *Conducting Polymer Hybrids, Springer Series on Polymer and Composite Materials*; Kumar, V., Kalia, S., Swart, H., Eds.; Springer: Cham, Switzerland, 2017; pp. 165–192.
16. Ramanavicius, S.; Ramanavicius, A. Conducting polymers in the design of biosensors and biofuel cells. *Polymers* **2021**, *13*, 49. [CrossRef]
17. Mahato, N.; Jang, H.; Dhyani, A.; Cho, S. Recent progress in conducting polymers for hydrogen storage and fuel cell applications. *Polymers* **2020**, *12*, 2480. [CrossRef]
18. Umoren, S.A.; Solomon, M.M. Protective polymeric films for industrial substrates: A critical review on past and recent applications with conducting polymers and polymer composites. *Progr. Mater. Sci.* **2019**, *104*, 380–450. [CrossRef]
19. Xu, H.; Zhang, Y. A review on conducting polymers and nanopolymer composite coatings for steel corrosion protection. *Coatings* **2019**, *9*, 807. [CrossRef]
20. Wong, Y.C.; Ang, B.C.; Haseeb, A.; Baharuddin, A.A.; Wong, Y.H. Conducting polymers as chemiresistive gas sensing materials: A review. *J. Electrochem. Soc.* **2020**, *167*, 037503. [CrossRef]
21. Fratoddi, I.; Venditti, I.; Cametti, C.; Russo, M.V. Chemiresistive polyaniline-based gas sensors: A mini review. *Sens. Actuators B* **2015**, *220*, 534–548.
22. Lakard, B. Electrochemical biosensors based on conducting polymers: A review. *Appl. Sci.* **2020**, *10*, 6614. [CrossRef]
23. El-Said, W.A.; Abdelshakour, M.; Choi, J.H.; Choi, J.W. Application of conducting polymer nanostructures to electrochemical biosensors. *Molecules* **2020**, *25*, 307. [CrossRef] [PubMed]
24. Talikowska, M.; Fu, X.; Lisak, G. Application of conducting polymers to wound care and skin tissue engineering: A review. *Biosens. Bioelectron.* **2019**, *135*, 50–63. [CrossRef]
25. Guo, B.; Ma, P.X. Conducting polymers for tissue engineering. *Biomacromolecules* **2018**, *19*, 1764–1782. [CrossRef]
26. Grazulevicius, J.V.; Strohriegl, P.; Pielichowski, J.; Pielichowski, K. Carbazole containing polymers: Synthesis, properties and applications. *Prog. Polym. Sci.* **2003**, *28*, 1297–1353. [CrossRef]
27. Alem, S.; Graddage, N.; Lu, J.; Kololuoma, T.; Movileanu, R.; Tao, Y. Flexographic printing of polycarbazole-based inverted solar cells. *Org. Electron.* **2018**, *52*, 146–152. [CrossRef]
28. Burgués-Ceballos, I.; Hermerschmidt, F.; Akkuratov, A.V.; Susarova, D.K.; Troshin, P.A.; Choulis, S.A. High-Performing Polycarbazole Derivatives for Efficient Solution-Processing of Organic Solar Cells in Air. *ChemSusChem* **2015**, *8*, 4209–4215. [CrossRef]
29. Bovill, E.; Yi, H.; Iraqi, A.; Lidzey, D.G. The fabrication of polyfluorene and polycarbazole-based photovoltaic devices using an air-stable process route. *Appl. Phys. Lett.* **2014**, *105*, 223302. [CrossRef]
30. Kocaeren, A.A. Electrochemical synthesis and electrochromic application of a novel polymer based on carbazole. *Org. Electron.* **2015**, *24*, 219–226. [CrossRef]

31. Soganci, T.; Baygu, Y.; Gök, Y.; Ak, M. Disulfide-linked symmetric N-alkyl carbazole derivative as a new electroactive monomer for electrochromic applications. *Synth. Met.* **2018**, *244*, 120–127. [CrossRef]
32. Chen, C.H.; Wang, Y.; Michinobu, T.; Chang, S.W.; Chiu, Y.C.; Ke, C.Y.; Liou, G.S. Donor-Acceptor Effect of Carbazole-Based Conjugated Polymer Electrets on Photoresponsive Flash Organic Field-Effect Transistor Memories. *ACS Appl. Mater. Interfaces* **2020**, *12*, 6144–6150. [CrossRef]
33. Rice, N.A.; Bodnaryk, W.J.; Mirka, B.; Melville, O.A.; Adronov, A.; Lessard, B.H. Polycarbazole-Sorted Semiconducting Single-Walled Carbon Nanotubes for Incorporation into Organic Thin Film Transistors. *Adv. Electron. Mater.* **2019**, *5*, 1800539. [CrossRef]
34. Grigoras, A.G. A review on medical applications of poly(N-vinylcarbazole) and its derivatives. *Int. J. Polym. Mater. Polym. Biomater.* **2016**, *65*, 888–900. [CrossRef]
35. Pernites, R.; Ponnapati, R.; Felipe, M.J.; Advincula, R. Electropolymerization molecularly imprinted polymer (E-MIP) SPR sensing of drug molecules: Pre-polymerization complexed terthiophene and carbazole electroactive monomers. *Biosens. Bioelectron.* **2011**, *26*, 2766–2771. [CrossRef]
36. Morin, J.F.; Leclerc, M.; Adès, D.; Siove, A. Polycarbazoles: 25 Years of Progress. *Macromol. Rapid Commun.* **2005**, *26*, 761–778. [CrossRef]
37. Ates, M.; Uludag, N. Carbazole derivative synthesis and their electropolymerization. *J. Solid State Electrochem.* **2016**, *20*, 2599–2612. [CrossRef]
38. Karon, K.; Lapkowski, M. Carbazole electrochemistry: A short review. *J. Solid State Electrochem.* **2015**, *19*, 2601–2610. [CrossRef]
39. Boudreault, P.L.T.; Beaupré, S.; Leclerc, M. Polycarbazoles for plastic electronics. *Polym. Chem.* **2010**, *1*, 127–136. [CrossRef]
40. Michinobu, T.; Osako, H.; Shigehara, K. Synthesis and Properties of 1,8-Carbazole-Based Conjugated Copolymers. *Polymers* **2010**, *2*, 159–173. [CrossRef]
41. Liang, Y.K.; Ruan, B.F.; Tian, Y.P. Synthesis, crystal structure and in vitro antitumor activity of a novel organotin(IV) complex with 9-hexyl-9H-carbazole-3-carboxylic acid. *Russ. J. Coord. Chem.* **2012**, *38*, 396–401. [CrossRef]
42. Düdükcü, M.; Udum, Y.A.; Ergün, Y.; Köleli, F. Electrodeposition of Poly(4-methyl carbazole-3-carboxylic acid) on Steel Surfaces and Corrosion Protection of Steel. *J. Appl. Polymer. Sci.* **2009**, *111*, 1496–1500. [CrossRef]
43. Elkhidr, H.E.; Ertekin, Z.; Udum, Y.A.; Pekmez, K. Electrosynthesis and characterizations of electrochromic and soluble polymer films based on N- substituted carbazole derivates. *Synth. Met.* **2020**, *260*, 116253. [CrossRef]
44. Kuo, C.W.; Hsieh, T.H.; Hsieh, C.K.; Liao, J.W.; Wu, T.Y. Electrosynthesis and characterization of four electrochromic polymers based on carbazole and indole-6-carboxylic acid and their applications in high-contrast electrochromic devices. *J. Electrochem. Soc.* **2014**, *161*, D782. [CrossRef]
45. Zhang, Y.; Chen, S.; Zhang, Y.; Du, H.; Zhao, J. Design and Characterization of New D–A Type Electrochromic Conjugated Copolymers Based on Indolo[3,2-b]Carbazole, Isoindigo and Thiophene Units. *Polymers* **2019**, *11*, 1626. [CrossRef]
46. Aristizabal, J.A.; Soto, J.P.; Ballesteros, L.; Muñoz, E.; Ahumada, J.C. Synthesis, electropolymerization, and photoelectrochemical characterization of 2,7-di(thiophen-2-yl)-N-methylcarbazole. *Polym. Bull.* **2012**, *70*, 35–46. [CrossRef]
47. Aristizabal, J.A.; Ahumada, J.C.; Soto, J.P. Electrochemical preparation and characterization of a new conducting copolymer of 2,7-carbazole and 3-octylthiophene. *Polym. Bull.* **2017**, *74*, 1649–1660. [CrossRef]
48. Guzel, M.; Karatas, E.; Ak, M. A new way to obtain black electrochromism: Appropriately covering whole visible regions by absorption spectra of copolymers composed of EDOT and carbazole derivatives. *Smart Mater. Struct.* **2019**, *28*, 025013. [CrossRef]
49. Aydin, A.; Kaya, I. Syntheses of novel copolymers containing carbazole and their electrochromic properties. *J. Electroanal. Chem.* **2013**, *691*, 1–12. [CrossRef]
50. Lakard, S.; Contal, E.; Mougin, K.; Magnenet, C.; Lakard, B. Electrochemical preparation and physicochemical study of polymers obtained from carbazole and N-((methoxycarbonyl)methyl)carbazole. *Synth. Met.* **2020**, *270*, 116584. [CrossRef]
51. Contal, E.; Sougueh, C.M.; Lakard, S.; Et Taouil, A.; Magnenet, C.; Lakard, B. Investigation of polycarbazoles thin films prepared by electrochemical oxidation of synthesized carbazole derivatives. *Front. Mater.* **2019**, *6*, 131. [CrossRef]
52. Pittenger, B.; Erina, N.; Su, C. Mechanical Property Mapping at the Nanoscale Using PeakForce QNM Scanning Probe Technique. In *Nanomechanical Analysis of High Performance Materials*; Solid Mechanics and Its Applications; Tiwari, A., Ed.; Springer: Dordrecht, The Netherlands, 2014; Volume 203, pp. 31–51.
53. Stewart, J.J.P. Optimization of parameters for semiempirical methods I. Method. *J. Comput. Chem.* **1989**, *10*, 209–220. [CrossRef]
54. Becke, A.D. A new mixing of Hartree-Fock and local density-functional theories. *J. Chem. Phys.* **1993**, *98*, 1372–1377. [CrossRef]
55. Lee, C.; Yang, W.; Parr, R.G. Development of the Colle-Salvetti correlation-energy formula into a functional of the electron density. *Phys. Rev. B* **1988**, *37*, 785–789. [CrossRef]
56. McCormick, T.M.; Bridges, C.R.; Carrera, E.I.; DiCarmine, P.M.; Gibson, G.L.; Hollinger, J.; Kozycz, L.M.; Seferos, D.S. Conjugated Polymers: Evaluating DFT Methods for More Accurate Orbital Energy Modeling. *Macromolecules* **2013**, *46*, 3879–3886. [CrossRef]
57. Zhuang, W.; Bolognesi, M.; Seri, M.; Henriksson, P.; Gedefaw, D.; Kroon, R.; Jarvid, M.; Lundin, A.; Wang, E.; Muccini, M.; et al. Influence of Incorporating Different Electron-Rich Thiophene-Based Units on the Photovoltaic Properties of Isoindigo-Based Conjugated Polymers: An Experimental and DFT Study. *Macromolecules* **2013**, *46*, 8488–8499. [CrossRef]
58. Nayyar, I.H.; Batista, E.R.; Tretiak, S.; Saxena, A.; Smith, D.L.; Martin, R.L. Localization of Electronic Excitations in Conjugated Polymers Studied by DFT. *J. Phys. Chem. Lett.* **2011**, *2*, 566–571. [CrossRef]
59. Ambrose, J.F.; Nelson, R.F. Anodic oxidation pathways of carbazoles (I. Carbazole and N-substituted derivatives). *J. Electrochem. Soc.* **1968**, *115*, 1159–1163. [CrossRef]

60. Ravindranath, R.; Ajikumar, P.K.; Bahulayan, S.; Hanafiah, N.B.; Baba, A.; Advincula, R.C.; Knoll, W.; Valiyaveettil, S. Ultrathin conjugated polymer network films of carbazole functionalized poly(p-phenylenes) via electropolymerization. *J. Phys. Chem. B* **2007**, *111*, 6336–6343. [CrossRef]
61. Lapkowski, M.; Zak, J.; Karon, K.; Marciniec, B.; Prukała, W. The mixed carbon–nitrogen conjugation in the carbazole based polymer; the electrochemical, UV Vis, EPR, and IR studies on 1,4-bis[(E)2-(9H-carbazol-9-yl)vinyl]benzene. *Electrochim. Acta* **2011**, *56*, 4105–4111.
62. Asavapiriyanont, S.; Chandler, G.K.; Gunawardena, G.A.; Pletcher, D. The electrodeposition of polypyrrole films from aqueous solutions. *J. Electroanal. Chem.* **1984**, *177*, 229–244. [CrossRef]
63. Hillman, A.R.; Mallen, E.F. Nucleation and growth of polythiophene films on gold electrodes. *J. Electroanal. Chem.* **1987**, *220*, 351–367. [CrossRef]
64. Hamnett, A.; Hillman, A.R. An ellipsometric study of the nucleation and growth of polythiophene films. *J. Electrochem. Soc.* **1988**, *135*, 2517–2524. [CrossRef]